Hydrol. Earth Syst. Sci. Discuss., doi:10.5194/hess-2016-244, 2016
Manuscript under review for journal Hydrol. Earth Syst. Sci.
Published: 26 May 2016

Hydrology and Earth System Sciences
Open Access
Discussions

The effect of chalk representation in land surface modelling

Mostaquimur Rahman[1], Rafael Rosolem[1,2]

[1]Department of Civil Engineering, University of Bristol, Bristol, UK

[2]Cabot Institute, University of Bristol, Bristol, UK

Abstract

Modelling and monitoring of hydrological processes in the unsaturated zone of the chalk, which is a porous medium with fractures, is important to optimize water resources assessment and management practices in the United Kingdom (UK). However, efficient simulations of water movement through chalk unsaturated zone is difficult mainly due to the fractured nature of chalk, which creates high-velocity preferential flow paths in the subsurface. Complex hydrology in the chalk aquifers may also influence land surface mass and energy fluxes because processes in the hydrological cycle are connected via non-linear feedback mechanisms. In this study, it is hypothesized that explicit representation of chalk hydrology in a land surface model influences land surface processes by affecting water movement through the shallow subsurface. In order to substantiate this hypothesis, a macroporosity parameterization is implemented in the Joint UK Land Environment Simulator (JULES), which is applied on a study area encompassing the Kennet catchment in the Southern UK. The simulation results are evaluated using field measurements and satellite remote sensing observations of various fluxes and states in the hydrological cycle (e.g., soil moisture, runoff, latent heat flux) at two distinct spatial scales (i.e., point and catchment). The results reveal the influence of representing chalk hydrology on land surface mass and energy balance components such as surface runoff and latent heat flux via subsurface processes (i.e., soil moisture dynamics) in JULES, which corroborates the proposed hypothesis.

Keywords: Chalk hydrology, macroporosity, land surface modelling, bulk conductivity model.

1. Introduction

Chalk can be described as a fine-grained porous medium traversed by fractures [*Price et al.*, 1993]. The unsaturated zone of chalk aquifers play an important role on various important processes (e.g., recharge) of the hydrological cycle in the UK [e.g., *Lee et al.*, 2006; *Ireson et al.*, 2009]. Therefore, both monitoring [e.g., *Bloomfield*, 1997; *Ireson et al.*, 2006] and modelling [e.g., *Brouyère*, 2006; *Ireson and Butler*, 2011, 2013; *Sorensen et al.*, 2014] strategies have been adapted previously to understand the governing hydrological processes in the chalk unsaturated zone.

In chalk, the matrix provides porosity and storage capacity, while the fractures greatly enhance permeability [*Van den Daele et al.*, 2007]. Water movement through chalk matrix is slow due to its relatively high porosity (0.3-0.4) and low permeability (10^{-9}-10^{-8} ms^{-1}). A fractured chalk system, in contrast, conducts water at a considerably higher velocity because of relatively high permeability (10^{-5}-10^{-3} ms^{-1}) and low porosity (of the order 10^{-4}) of fractures [*Price et al.*, 1993].

Simulating water flow through the matrix-fracture system of chalk has been the subject of research for some time. Both conceptual [e.g., *Price et al.*, 2000; *Haria et al.*, 2003] and physics-based [e.g., *Mathius et al.*, 2006; *Ireson et al.*, 2009] models have been proposed previously to describe water flow through chalk unsaturated zone. The physics-based models mentioned above were developed based on dual-continua approach and required relatively large number of parameters that were calibrated via inverse modelling using observed soil moisture and matric potential data.

The aforementioned studies revealed the importance of representing the matrix-fracture flow nature in simulating subsurface hydrological processes in chalk-dominated aquifers. In recent years, representation of chalk has also gained attention in land surface modelling. *Gascoin et*

Hydrol. Earth Syst. Sci. Discuss., doi:10.5194/hess-2016-244, 2016
Manuscript under review for journal Hydrol. Earth Syst. Sci.
Published: 26 May 2016

al. [2009] applied the Catchment Land Surface Model (CLSM) over the Somme River basin in northern France. A linear reservoir was included in the TOPMODEL based runoff formulation of CLSM to account for the contribution of chalk aquifers to river discharge. *Le Vine et al.* [2016] applied the Joint UK Land Environment Simulator (JULES [*Best et al.*, 2011]) over the Kennet catchment in southern England to evaluate the hydrological limitations of land surface models. In that study, two intersecting Brooks and Corey curve was proposed, which allowed a dual curve soil moisture retention representation for the two distinct flow domains of chalk (i.e., matrix and fracture) in the model. Considering this dual Brooks and Corey curve, a three-dimensional groundwater flow model (ZOOMQ3D [*Jackson and Spink*, 2004]) was coupled to JULES to demonstrate the strong influence of representing chalk hydrology and groundwater flow on simulated soil moisture and runoff.

The above mentioned studies suggest that the representation of chalk affects the hydrological processes simulated by land surface models. Because the processes of the hydrological cycle are connected via non-linear feedback mechanisms [e.g., *Kollet and Maxwell*, 2008; *Rahman et al.*, 2014], the representation of water flow through the matrix-fracture system of chalk may also influence simulated land surface energy fluxes (e.g., latent heat flux), which has not yet been explicitly discussed. In this context, our hypothesis is that a consistent representation of water movement through chalk in a land surface model affects the exchange of mass and energy fluxes at the surface, which may be important to consider in water resources assessment and management practices (e.g., flood and drought prediction over chalk-dominated areas). In order to substantiate this hypothesis, a macroporosity parameterization, namely the *Bulk Conductivity* (BC) model is implemented in JULES and evaluated at two distinct spatial scales (i.e., point and catchment). At the point-scale, the BC model is evaluated against observed soil moisture data. The proposed model is then applied over the Kennet catchment in the Southern England and the fluxes and states of the hydrological cycle

Hydrol. Earth Syst. Sci. Discuss., doi:10.5194/hess-2016-244, 2016
Manuscript under review for journal Hydrol. Earth Syst. Sci.
Published: 26 May 2016

are simulated for multiple years to demonstrate the importance of representing chalk hydrology, which supports the proposed hypothesis.

2. A model of flow through chalk unsaturated zone

In this study, the *Bulk Conductivity* (BC) model based on the work by *Zehe et al.* [2001] is incorporated to represent the flow of water through the fractured chalk unsaturated zone. According to this approach, if the relative saturation (S) exceeds a certain threshold (S_0) at a soil grid, the saturated hydraulic conductivity (K_s) is increased to a bulk saturated hydraulic conductivity (K_{sb}) as follows

$$K_{sb} = K_s + K_s f_m \frac{S-S_0}{1-S_0} \qquad \text{if } S > S_0 \qquad (1)$$

with $S = \frac{\theta-\theta_r}{\theta_s-\theta_r}$

where f_m is a macroporosity factor (-), θ is soil moisture (m^3m^{-3}), θ_s is soil moisture at saturation (m^3m^{-3}), and θ_r is the residual soil moisture (m^3m^{-3}). Note that S ranges from zero in case of completely dry soils to one for fully wet soils.

Equation 1 indicates that the onset of water flow through the fracture system of chalk is controlled by the threshold S_0. According to *Wellings and Bell* [1980], water flow through fractures dominates over matrix flow in chalk when the pressure head in soil becomes higher than -0.50 mH_2O. In this study, $S_0 = 0.80$, which is based on observed soil moisture-matric potential relationship in the study area (Figure S1).

In *Zehe et al.* [2001], f_m was defined as the ratio of the saturated water flow rate in all macropores in a model element to the corresponding value in soil matrix, which can be determined based on density and length of fractures at small scales. In addition, f_m has also been considered as a calibration parameter previously [e.g., *Blume*, 2008; *Zehe et al.*, 2013]. In this study, we define f_m as a characteristic soil property reflecting the influence of fractures

Hydrol. Earth Syst. Sci. Discuss., doi:10.5194/hess-2016-244, 2016
Manuscript under review for journal Hydrol. Earth Syst. Sci.
Published: 26 May 2016

on soil water movement [*Zehe and Blöschl*, 2004], and estimate it from the relative difference of permeability between chalk matrix and fractured chalk system that can be of the order 10^5 according to *Price et al.* [1999]. Consequently, we consider a macroporosity factor of $f_m = 10^5$ in this study.

3. Methods

3.1. Study area

The study area encompasses the Kennet catchment located in the Southern England with an area of about 1033 km^2 (Figure 1a). Kennet, in general, is rural in nature with scattered settlements and has a maximum altitude of approximately 297 m (Above Ordnance Level). River Kennet discharges into the North Sea through London. Major tributaries of this river are Lambourn, Dun, Enborne, and Foudry Brook. An average annual rainfall of approximately 760 mm was recorded in the catchment over a 40 year period from 1961-1990.

Solid geology of the Kennet catchment is dominated by chalk, which is overlain by thin soil layer. While lower chalk outcrops along the northern catchment boundary, progressively younger rocks are found in the southern part. In general, surface runoff production is very limited over the regions of the catchment where chalk outcrops. The flow regime shows a distinct characteristics of slow response to groundwater held within the chalk aquifer [*Le Vine et al.*, 2016]. According to *Ireson and Butler* [2013], the unsaturated zone of chalk shows slow drainage over summer and bypass flow during wet periods in this catchment.

3.2. Field measurements and remotely sensed data

Table 1 summarizes the field measurements and remote sensing data used in this study. We use in-situ soil moisture and runoff measurements along with remotely sensed latent heat flux (*LE*) data to assess model performance in simulating the mass and energy balance components of the hydrological cycle. Point scale soil moisture measurements at two

Hydrol. Earth Syst. Sci. Discuss., doi:10.5194/hess-2016-244, 2016
Manuscript under review for journal Hydrol. Earth Syst. Sci.
Published: 26 May 2016

Hydrology and Earth System Sciences Discussions
Open Access

adjacent sites (~20 m apart) at the Warren Farm (Figure 1) were provided by Centre for Ecology and Hydrology (CEH). A Didcot neutron probe was used at these locations to measure fortnightly soil moisture at different depths below land surface (10 cm apart down to 0.8 m, 20 cm apart between 0.8-2.2 m, and 30 cm apart between 2.2-4 m) [*Hewitt et al.*, 2010].

The National River Flow Archive (NRFA) coordinates discharge measurements from gauging station networks across UK. These networks are operated by Environmental Agency (England), Natural Resources Wales, the Scottish Environment Protection Agency, and Rivers Agency (Northern Ireland). We use discharge measurement provided by NRFA to calculate the runoff ratio over the Kennet catchment in this study.

The MOD16 product of the Moderate Resolution Imaging Spectroradiometer (MODIS) is a part of NASA/EOS project that provides estimation of global terrestrial *LE*. The *LE* estimation from MOD16 is based on remotely sensed land surface data [e.g., *Mu et al.*, 2007]. In this study, 8-day and monthly *LE* data products from MODIS is used to evaluate the model's performance in simulating land surface energy fluxes.

3.3. Land surface model

In this study, we use the Joint UK Land Environment Simulator (JULES [e.g., *Best et al.*, 2011; *Clark et al.*, 2011]) version 4.2. JULES is a flexible modelling platform with a modular structure aligned to various physical processes developed based on the Met Office Surface Exchange Scheme (MOSES [e.g., *Cox et al.*, 1999; *Essery et al.*, 2003]). Meteorological data including precipitation, incoming short- and longwave radiation, temperature, specific humidity, surface pressure, and wind speed are required to drive JULES. Each grid box in JULES can comprise nine surface types (broadleaf trees, needle leaf trees, C3 grass, C4 grass,

Hydrol. Earth Syst. Sci. Discuss., doi:10.5194/hess-2016-244, 2016
Manuscript under review for journal Hydrol. Earth Syst. Sci.
Published: 26 May 2016

shrubs, inland water, bare soil, and ice) represented by respective fractional coverage. Each surface type is represented by a tile and a separate energy balance is calculated for each tile.

Subsurface heat and water transport equations are solved based on finite-difference approximation in JULES as described in *Cox et al.* [1999]. Moisture transport in the subsurface is described by the finite difference form of Richards' equation. The vertical soil moisture flux is calculated using the Darcy's law. While the top boundary condition to solve Richards' equation is infiltration at soil surface, the bottom boundary condition in JULES is free drainage that contributes to subsurface runoff.

Surface runoff is calculated by combining the equations of throughfall and grid box average infiltration in JULES. In order to direct the generated runoff to a channel network, river routing is implemented based on the discrete approximation of one-dimensional kinematic wave equation [e.g., *Bell et al.*, 2007]. In this approach, river network is derived from the digital elevation model (DEM) of the study area and different wave speeds are applied to surface and subsurface runoff components and channel flows [e.g., *Bell and Moore*, 1998]. A return flow term accounts for the transfer of water between subsurface and land surface [e.g., *Dadson et al.*, 2010, 2011].

3.4. Model configurations and input data

3.4.1. Point scale

At the point scale, JULES is configured to simulate the mass and energy fluxes at Warren Farm (Figure 1). A total subsurface depth of 5 m is considered in the model with a vertical discretization ranging from 10 cm at the land surface to 50 cm at the bottom of the model domain. Note that this discretization is consistent with the soil moisture measurement depths mentioned in section 3.2. The vegetation type is implemented as C3 grass using the default parameters in JULES. The soil hydraulic properties are estimated based on texture (Table 2), which is predominantly loamy at Warren Farm. The saturation-pressure head relationship is described using the Van Genuchten [*Van Genuchten*, 1980] model with parameter values (Table 2) obtained from *Schaap and Leij* [1998] in the model.

Point scale simulations were performed over 2 consecutive years from 2003-2005 at an hourly time step. Except for precipitation, hourly atmospheric forcing data to drive JULES was obtained from an automatic weather station operated by the CEH at Warren Farm. In order to estimate hourly precipitation data to run JULES, rain gauge measurements by the Met Office [*Met Office*, 2006] were used. Inverse distance interpolation technique [e.g. *Garcia et al.*, 2008; *Ly et al.*, 2013] was applied on rainfall measurements from 13 gauges closest to Warren Farm (distance varies from 25-60 km) to obtain hourly precipitation for the point scale simulations.

3.4.2. Catchment scale

At the catchment scale, JULES is configured over the study area (Figure 1) with a uniform lateral grid resolution of 1 km with 70 x 40 cells in x and y dimensions, respectively. The vertical discretization is identical to that of the point scale simulations described in the previous section. Spatially distributed vegetation type information for the study area (Figure 1b) is obtained from the Land Cover Map 2007 (LCM2007) dataset [e.g., *Morton et al.*, 2011]. Harmonized World Soil Database (HWSD) from the Food and Agricultural Organization of UNO (FAO) is used to obtain the texture of different soil types in the region (Figure 1c). Van Genuchten model, with parameter values (Table 2) obtained from *Schaap and Leij* [1998] is used to represent the saturation-pressure head relationship for different soil types, which is identical to the point scale simulations.

Simulations were performed over 5 consecutive years from 2006-2011 at the catchment scale. Note that the simulation periods of catchment and point scale (2003-2005) does not coincide due to the availability of soil moisture measurements described in section 3.2. Spatially distributed meteorological data from the Climate, Hydrology, and Ecology research Support System (CHESS) was used to obtain the atmospheric forcing to drive JULES. The CHESS data includes 1 km resolution gridded daily meteorological variables [*Robinson et al.*, 2015]. This daily data is downscaled using a disaggregation technique described in *Williams and Clark* [2014] to obtain hourly atmospheric forcing. The flow direction required for river routing is extracted from the USGS HydroSHEDS digital elevation data [*Lehner et al.*, 2008].

3.5. Setup of numerical experiments

We consider two different model configurations, namely, *default* and *macro* (Figure 2), to explore the influence of chalk hydrology on simulated land surface processes in JULES. The *default* configuration corresponds to the standard parameterizations of JULES that does not represent chalk hydrology in the model. In this configuration, each soil column in JULES is considered to be vertically homogeneous with the soil properties defined in Table 2, which is motivated by the Met Office JULES Global Land 4.0 configuration described in *Walters et al.* [2014]. The *macro* configuration, in contrast, explicitly represents chalk hydrology in the model. The *macro* setup modifies the *default* configuration by applying chalk hydraulic properties (Table 3) from 30 cm below land surface to the bottom of the model domain (i.e. 500 cm). The BC model is applied in the chalk layers (30-500 cm) to simulate water flow in the *macro* configuration. Therefore, soil columns in the model can be divided into topsoil (0-30 cm) and chalk (30-500 cm) in *macro*. Note that except for this inclusion of chalk, *default* and *macro* configurations are identical in terms of model set up and input data.

The topsoil depth of 30 cm is defined based on several augured soil samples collected during a field campaign at Warren Farm in 2015 (Figure 2). This depth is corroborated by additional information from the British Geological Survey (BGS) operated borehole records

Hydrol. Earth Syst. Sci. Discuss., doi:10.5194/hess-2016-244, 2016
Manuscript under review for journal Hydrol. Earth Syst. Sci.
Published: 26 May 2016

(http://www.ukso.org/pmm/soil_depth_samples_points.html), which show that topsoil depths vary from 10-40 cm over the study area. We therefore apply the *macro* configuration assuming a spatially homogeneous 30 cm topsoil depth for both point and catchment scale simulations.

4. Results and discussion

4.1. Point scale simulations

Figure 3 shows observed and simulated volumetric soil moisture from the *default* model configuration at Warren Farm from 2003-2005. This figure shows that simulated soil moisture at shallow soil layers (up to 50 cm) compares reasonably well with the observed data. However, in the deeper layers, the model considerably underestimates soil moisture. Figure 4 compares observed and simulated volumetric soil moisture from the *macro* configuration at Warren Farm over the simulation period. This figure shows that especially in the deeper soil layers, the agreement between observed and simulated soil moisture improves remarkably relative to the *default* configuration throughout the simulation period. Notice again that the *default* and *macro* configurations are identical in terms of model setup and inputs except for the consideration of chalk. Therefore, the differences in soil moisture simulations between the two model configurations can be attributed to the representation of chalk hydrology in JULES.

Figure 5 presents the relative bias ($\Delta\mu$, see Appendix) of simulated soil moisture from the two model configurations at Warren Farm for various depth ranges. In the soil layers (0-30 cm), both *default* and *macro* configurations reproduces soil moisture reasonably well with the latter showing slightly better agreement with observations. However, in the chalk layers (30-500 cm), *default* fails to reproduce the soil moisture dynamics efficiently, simulating substantially dry conditions, which are observed from the mean relative bias ($\Delta\mu_{mean}$) of

$\Delta\mu_{mean} > 0.28$ for this configuration. In contrast, the *macro* configuration remarkably improves the agreement with the observed soil moisture profile in the chalk layers with the largest calculated $\Delta\mu_{mean} = -0.02$. Therefore, the inclusion of the BC model in JULES appears to improve the performance of overall soil moisture simulation at Warren Farm especially in the chalk layers.

In order to explore the reason of the discrepancies between simulated soil moisture from the two model configurations, Figure 6 shows S and water flux (w_f) profiles along with drainage through the bottom boundary (d_b) of *default* and *macro* for the entire simulation period. Figure 6b plots the contours of daily accumulated w_f through chalk (30-500 cm) over daily average S for the *macro* configuration (S_{macro}). Figure 6c shows S ($S_{default}$) and w_f through the same profile for the *default* configuration. A comparison between Figure 6b and 6c reveals that *default* is considerably drier compared to *macro* ($S_{default} < S_{macro}$) throughout the profile, which is consistent with Figure 5. Figure 6b shows notable flux through the profile following strong precipitation events (Figure 6a), indicating fast water flow through subsurface in the *macro* configuration (especially in winter). The *default* configuration, on the other hand, shows relatively slower movement of water in the subsurface (Figure 6c).

According to the BC model, fracture flow in chalk is activated in a soil grid if S exceeds S_0 (defined as 0.80), which is achieved predominantly during winter following strong precipitation events because of the prevailing wet conditions. Therefore, the activation of fracture flow explains the fast water movement patterns after strong precipitation events observed in Figure 6b. This result is consistent with *Ireson et al.* [2009], who showed that fracture flow through chalk dominates at Warren Farm during wet periods. Compared to the *macro* configuration, *default* does not show fast water flow to the deeper soil layers because the latter does not represent the matrix-fracture flow nature of chalk in JULES.

Hydrol. Earth Syst. Sci. Discuss., doi:10.5194/hess-2016-244, 2016
Manuscript under review for journal Hydrol. Earth Syst. Sci.
Published: 26 May 2016

Figure 6d compares daily sum of d_b from the two configurations. The *macro* configuration generally shows lower drainage compared to *default* with an exception in March 2003. Because of the gravity drainage lower boundary condition, water flow through the bottom of the model domain depends on K_s at the deepest soil layer in JULES. In chalk (*macro* configuration), K_s at the deepest soil layer is smaller compared to *default* (loam soil) especially when $S_0 < 0.8$ (Equation 1), which explains the lower drainage flux in case of the *Chalk* configuration. The reason of higher d_b in *macro* compared to *default* in March 2003 is the strong precipitation events (Figure 6a) causing considerable fracture flow and $S > 0.8$ at the bottom of the model domain (Figure 6b).

Figure 6 outlines the differences in simulated subsurface processes by the two model configurations. Fracture flow in chalk is activated according to the BC approach during wet periods that allows recharge at deeper soil layers in *macro*, which is absent in case of the *default* configuration. Moreover, the *default* configuration generally shows higher drainage flux through the lower boundary compared to *macro*. The combination of relatively low recharge and high drainage through lower boundary is the reason of the drier conditions simulated by *default*. In contrast, the *macro* configuration is characterized by fast recharge at the deeper soil layers through fractures and slow drainage through the bottom because of considerably lower K_s compared to *default*, which is the reason of relatively higher simulated soil moisture by this configuration that compares well with observations.

Several previous studies have discussed the influence of root zone soil moisture on land surface mass and energy balance components [e.g., *Wetzel and Chang*, 1987; *Chen and Hu*, 2004]. Therefore, the differences in soil moisture from two configurations discussed above may affect the land surface mass and energy fluxes in the model. In order to investigate this effect, Figure 7 shows the difference between daily average latent heat flux (*LE*) time series from *default* and *macro* configurations ($LE_{default}$ and LE_{macro}, respectively) at Warren Farm over the simulation period. This figure shows that the *default* configuration generally simulates lower *LE* compared to *macro* especially in the warmer months of the year.

The underestimation of *LE* in Figure 7 can be attributed to the differences in simulated soil moisture by the two configurations (Figure 3 and 4). In winter, abundant soil moisture is available in both *default* and *macro* to meet the relatively low evapotranspiration (ET) demand due to the prevailing energy-limited conditions. Therefore, Figure 7 shows negligible differences between $LE_{default}$ and LE_{macro} in winter. However, in summer, the discrepancies between soil moisture from the two model configurations result in marked differences between $LE_{default}$ and LE_{macro} because of the increased ET demand, which is consistent with previous studies [e.g., *Rahman et al.*, 2016].

In this section, subsurface and land surface processes simulated by *default* and *macro* configurations are discussed at the point scale. The simulation results show notable differences in soil moisture and *LE* from the two configurations. Because the only difference between *default* and *macro* configurations is the representation of the chalk hydrology, it appears that a consistent representation of chalk in JULES affects land surface processes via subsurface hydrodynamics supporting our hypothesis. In the next section, we test this hypothesis regionally by evaluating the mass and energy fluxes of the hydrological cycle at the catchment scale.

4.2. Catchment scale simulations

Figure 8 plots spatially averaged 8-day composites of *LE* from MODIS (LE_{MOD}) against $LE_{default}$ and LE_{macro} over the Kennet catchment. In this figure, the agreement between simulated *LE* and LE_{MOD} is evaluated using the coefficient of determination (R^2, see Appendix) that outlines the differences between *LE* simulated by the two model configurations. Comparison between $LE_{default}$ and LE_{MOD} shows a coefficient of determination of $R^2_{default}$ = 0.78. The agreement between simulated *LE* and LE_{MOD} improves in case of *macro* configuration, which is reflected by an increased coefficient of determination of R^2_{macro} = 0.82.

Figure 8 shows differences between $LE_{default}$ and LE_{macro} especially for relatively high *LE*, indicating discrepancies especially during the warmer months of the year. Figure 9a presents spatially averaged time series of monthly LE_{MOD}, $LE_{default}$ and LE_{macro}. This figure shows negligible differences in *LE* from the two configurations during the colder months of the year, while differences between $LE_{default}$ and LE_{macro} increases substantially in summer. Consequently, the *default* configuration underestimates *LE* especially in summer compared to LE_{MOD}, which is improved when chalk hydrology is explicitly considered in JULES in the *macro* configuration.

Figure 9b plots spatially averaged time series of daily $S_{default}$ and S_{macro} over the Kennet catchment. Note that average *S* at the first 8 vertical model layer (0-100 cm below land surface) is presented in this figure, which highlights the difference in root zone moisture content from the two model configurations. Figure 9b shows relatively lower *S* simulated by the *default* configuration compared to S_{macro}. In JULES, *LE* depends on surface conductance to evaporation, which is controlled by the mean soil moisture in the root zone. Therefore, the differences in $S_{default}$ and S_{macro} is consistent with the underestimation of *LE* by the *macro* configuration (Figure 9a). Note that despite the differences in *S* between the two configurations over the entire simulation period, Figure 9a shows significant *LE* differences only in summer. This is due to the prevailing energy limited conditions during the colder months over the region, which was discussed in the previous section. Figure 9 suggest that representing chalk hydrology in JULES considerably influences simulated *LE* by modifying shallow soil moisture at the catchment scale, also supporting our hypothesis.

Table 4 compares observed and simulated daily average runoff from the two model configurations over the Kennet catchment from 2006-2011. The runoff ratio (*RR*, see Appendix), which is equal to the mean volume of flow divided by the volume of precipitation [e.g., *Kelleher et al.*, 2015], assesses the partitioning of precipitation into runoff over the catchment. The *default* configuration (*RR* = 0.82) shows considerably higher *RR* compared to observation (*RR* = 0.40), indicating overestimation of runoff by the model. Including chalk hydrology in the model remarkably improves the agreement between observed and simulated mean runoff over the Kennet catchment, which is assessed from a runoff ratio of *RR* = 0.38 for the *macro* configuration.

In Table 4, the relative bias (Δμ) of 1.04 between observed and simulated runoff from the *default* configuration again indicates the overestimation by the model. In comparison, *macro* shows a relative bias (Δμ = -0.07), indicating improvement between observed and simulated mean runoff volume compared to *default*. The relative difference in standard deviation (Δσ, see Appendix) compares the magnitude of observed and simulated runoff in Table 3. This comparison shows that the *default* configuration overestimates the variability of runoff over the Kennet catchment (Δσ = 2.04), which is improved in case of *macro* (Δσ = 0.56).

In JULES, moisture from soil and canopy water storage is depleted to meet the ET demand. Additionally, surface runoff generation depends on canopy water storage in the model [*Best et al.*, 2011]. Because of this connection between ET and surface runoff generation via canopy water storage, the differences in runoff demonstrated in Table 4 can be attributed to the disagreement between $LE_{default}$ and LE_{macro} demonstrated in Figure 9a. Therefore, it appears that *LE* in JULES is affected by the inclusion of chalk hydrology, which consequently influences surface runoff generation corroborating our hypothesis.

5. Summary and Conclusions

In this study, we hypothesized that a consistent representation of chalk hydrology affects land surface mass and energy balance components via subsurface hydrodynamics simulated by a land surface model. In order to support this hypothesis, the *Bulk Conductivity* (BC) model that simulates water flow through the matrix-fracture system of chalk was implemented in the Joint UK Land Environment Simulator (JULES). This model was applied on the Kennet catchment located in the southern UK to simulate the mass and energy fluxes of the hydrological cycle for multiple years. Two model configurations, namely *default* and *macro* were considered with the latter representing chalk hydrology in JULES using the BC model.

The proposed BC model is a single continuum approach of modelling preferential flow [e.g., *Beven and Germann*, 2013] that involves only 2 parameters, namely macroporosity factor (f_m) and relative saturation threshold (S_0). In addition, these parameters can be estimated from the physical properties of chalk in this study. Despite its simplicity, the BC model was able to reproduce the hydrological processes in chalk without model calibration, which was assessed by comparing the model results with observations. The discrepancies between the measured and simulated fluxes and states can be improved by a comprehensive model calibration, which is out of the scope of this study and should be the subject of future research.

The results showed that JULES generally underestimates root zone soil moisture without a consistent representation of chalk hydrology. Consequently, *LE* is underestimated by the model without chalk representation. The effect of chalk hydrology was also observed on runoff, which was attributed to the interconnection between *LE* and runoff generation in the model. Therefore, representing the matrix-fracture flow nature of chalk in a land surface model affects land surface processes via shallow soil moisture dynamics, which supports the proposed hypothesis.

Habtes et al. [2010] argued that flood flow in chalky catchments is influenced by the hydrological processes in the unsaturated zone. Implementing the BC model in JULES, this study showed that representing chalk hydrology significantly affects subsurface and land surface mass and energy fluxes. Therefore, the matrix-fracture flow nature of the aquifer may be important to consider in flood forecasting in chalk-dominated catchments.

Leeper et al. [2011] discussed the influence of shallow soil moisture on simulated atmospheric processes over karst landscapes because of the subsurface-land surface connection in the terrestrial system. In this study, we demonstrated that considering chalk hydrology considerably affects land surface mass and energy fluxes via subsurface hydrodynamics. This effect may be important to consider in numerical weather prediction models over the regions dominated by chalk because of the karst behaviour of chalk aquifers [e.g., *MacDonald et al.*, 1998; *Hartmann et al.*, 2014].

Le Vine et al. [2016] argued that the deep-groundwater system in a chalk-dominated catchment may influence the mass and energy balance components of the hydrological cycle, which is not considered in this study. The reason for that is JULES simulates water flow at shallow subsurface considering free drainage lower boundary condition and does not allow lateral movement of water between the soil columns. The effect of groundwater dynamics can be represented in JULES by coupling a three-dimensional groundwater flow model [e.g., *Le Vine et al.*, 2016; *Maxwell and Miller*, 2005], which will be addressed in future.

Acknowledgements

We gratefully acknowledge the support by the "A MUlti-scale Soil moisture Evapotranspiration Dynamics study – AMUSED" project funded by Natural Environment Research Council (NERC) grant number NE/M003086/1. The authors would also like to thank Ned Hewitt and Jonathan Evans from the Centre for Ecology and Hydrology (CEH) for providing the data for the point-scale analyses at the Warren Farm. Finally, we would like to thank Miguel Rico Ramirez (University of Bristol) for helping preparing the precipitation data from the rain gauge network used for the point-scale simulations, Thorsten Wagener (University of Bristol) for his valuable suggestions on model diagnostics, and Joost Iwema (University of Bristol) for helping with the soil samples collected during the 2015 field work campaign.

Appendix

Definition of Statistical Metrics

Coefficient of determination (R^2) for observation y = y1, …, yn and prediction f = f1, …, fn is defined as

$$R^2 = 1 - \frac{SS_{res}}{SS_{tot}}$$

where, SS_{res} is the residual sum of square and SS_{tot} is the total sum of square. SS_{res} and SS_{tot} are defined as

$$SS_{res} = \sum_{i=1}^{n}(y_i - f_i)^2 \quad \text{and}$$

$$SS_{tot} = \sum_{i=1}^{n}(y_i - \bar{y})^2 \quad \text{with } \bar{y} \text{ being the mean of y.}$$

Runoff ratio (RR) assesses the portion of precipitation that generates runoff over the catchment. RR is defined as

$$RR = \frac{\mu_{runoff}}{\mu_{rain}}$$

where μ_{runoff} is mean runoff and μ_{rain} is mean precipitation [e.g., *Kelleher et al.*, 2015].

Relative bias ($\Delta\mu$) between observed and simulated time series can be defined as

$$\Delta\mu = \frac{\mu_{mod} - \mu_{obs}}{\mu_{obs}}$$

where μ_{obs} and μ_{mod} are the mean of observed and simulated time series, respectively. While the optimal value of $\Delta\mu$ is zero, negative (positive) values indicate an underestimation (overestimation) by the model [e.g., *Gudmundsson et al.*, 2012].

Relative difference in standard deviation ($\Delta\sigma$) between observed and simulated time series can be defined as

$$\Delta\sigma = \frac{\sigma_{mod} - \sigma_{obs}}{\sigma_{obs}}$$

where σ_{obs} and σ_{mod} are the standard deviation of observed and simulated time series, respectively [e.g., *Gudmundsson et al.*, 2012].

References

Bell, V. A. and R. J. Moore (1998), A grid-based flood forecasting model for use with weather radar data: Part 1. Formulation, Hydrol. Earth Syst. Sc., 2, 265-281.

Bell, V. A., A. L. Key, R. G. Jones, and R. J. Moore (2007), Development of a high resolution grid-based river flow model for use with regional climate model output, Hydrol. Earth Syst. Sc., 11, 532-549.

Best, M. J., M. Pryor, D. B. Clark, G. G. Rooney, R. l. H. Essery, C. B. Ménard, J. M. Edwards, M. A. Hendry, A. Porson, N. Gedney, L. M. Mercado, S. Sitch, E. Blyth, O. Boucher, P. M. Cox, C. S. B. Grimmond, and R. J. Harding (2011), The Joint UK Land Environment Simulator (JULES), Model Description – Part 1: Energy and Water Fluxes, Geosci. Model Dev., 4, 677-699.

Beven, K., and P. Germann (2013), Macropores and water flow in soils revisited, Water Resour. Res., 49, 3071‐3092.

Bloomfield, J. (1997), The role of diagenesis in the hydrogeological stratification of carbonated aquifers: An example from the chalk at Fair Cross, Berkshire, UK, Hydrol. Earth Syst. Sc., 1, 19-33.

Blume, T. (2008), Hydrological processes in volcanic ash soils: measuring, modelling and understanding runoff generation in an undisturbed catchment, PhD thesis, Institut für Geoökologie, Universität Potsdam, Potsdam, Germany.

Brouyère, S. (2006), Modelling the migration of contaminants through variably saturated dual-porosity, dual-permeability chalk, J. Contam, Hydrol., 82, 195-219.

Chen, X., and Q. Hu (2004), Groundwater influences on soil moisture and surface evaporation, J. Hydrol., 297, 285‑300.

Clark, D. B., L. M. Mercado, S. Sitch, C. D. Jones, N. Gedney, M. J. Best, M. Pryor, G. G. Rooney, R. L. H. Essery, E. Blyth, O. Boucher, R. J. Harding, C. Huntingford, and P. M. Cox (2011), The Joint UK Land Environment Simulator (JULES), Model Description – Part 2: Carbon Fluxes and Vegetation Dynamics, Geosci. Model Dev. 4, 701-722.

Cox, P. M., R. A. Betts, C. B. Bunton, R. L. H. Essery, P. R. Rowntree and J. Smith (1999), The impact of new land surface physics on the GCM simulation of climate and climate sensitivity, Clim. Dynam., 15, 183-203.

Dadson, S. J., I. Ashpole, P. Harris, H. N. Davies, D. B. Clark, E. Blyth, and C. M. Taylor (2010), Wetland inundation dynamics in a model of land surface climate: Evaluation in the Niger inland delta region, J. Geophys. Res., 115.

Dadson, S. J., V. A. Bell, and R. G. Jones (2011), Evaluation of a grid based river flow model configured for use in a regional climate model, J. Hydrol., 411, 238-250.

Dettinger, M. D., and H. F. Diaz (2000), Global characteristics of streamflow seasonality and variability, J. Hydrometeorol., 1, 289-310.

Essery, R., M. Best, and P. Cox (2001), MOSES 2.2 technical documentation (Hadley Centre technical note 30), Hadley Centre, Met Office, UK.

Garcia, M., C. D. Peters-Lidard, and D. C. Goodrich (2008), Spatial interpolation of precipitation in a dense gauge network for monsoon storm events in the southwestern United States, Water Resour. Res., 44.

Hydrol. Earth Syst. Sci. Discuss., doi:10.5194/hess-2016-244, 2016
Manuscript under review for journal Hydrol. Earth Syst. Sci.
Published: 26 May 2016

Gascoin, S., A. Duchare, P. Ribstein, M. Carli, and F. Habtes (2000), Adaptation of a catchment-based land surface model to the hydrological setting of the Somme River basin (France), J. Hydrol., 368, 105-116.

Gudmundsson, L., T. Wagener, L. M. Tallaksen, and K. Engeland (2012), Evaluation of nine large-scale hydrological models with respect to the seasonal runoff climatology in Europe, Water Resour. Res., 48.

Gupta, H. V., H. Kling, K. K. Yilmaz, and G. F. Martinez (2009), Decomposition of the mean squared error and NSE performance criteria: implications for improving hydrological modelling, J. Hydrol., 377, 80-91.

Habtes, F., S. Gascoin, S. Korkmaz, D. Thiéry, M. Zribi, N. Amraoui, M. Carli, A. Ducharne, E. Leblois, E. Ledoux, E. Martin, J. Noilhan, C. Ottlé, and P. Viennot (2010), Multi-model comparison of a major flood in the groundwater-fed basin of the Somme River (France), Hydrol. Earth Syst. Sc., 14, 99-117.

Haria, A. H., M. G. Hodnett, and A. C. Johnson (2003), Mechanisms of groundwater recharge and pesticide penetration to chalk aquifer in southern England, J. Hydrol., 275, 122-137.

Hartmann, A., N. Goldscheider, T. Wagener, J. Lange, and M. Weiler (2014), Karst water resources in a changing world: Review of hydrological modeling approaches, Rev. Geophys., 52, 218–242, doi:10.1002/2013RG000443.

Hewitt, N., M. Robinson, and D. McNeil (2010), Pang and Lambourn hydrometric review 2009, Wallingford, NERC/Centre for Ecology and Hydrology, (CEH project number: C04076).

Ireson, A. M. and A. P. Butler (2011), Controls on preferential recharge to chalk aquifers, J. Hydrol., 398, 109-123.

Ireson, A. M. and A. P. Butler (2013), A critical assessment of simple recharge models: application to the UK chalk, Hydrol. Earth Syst. Sc., 17, 2083-2096.

Ireson, A. M., H. S. Wheater, A. P. Butler, S. A. Mathias, J. Finch, and J. D. Cooper (2006), Hydrological processes in the chalk unsaturated zone – insight from an intensive field monitoring program, J. Hydrol., 330, 29-43.

Ireson, A. M., S. A. Mathias, H. S. Wheater, A. P. Butler, and J. Finch (2009), A model for flow in the chalk unsaturated zone incorporating progressive weathering, J. Hydrol., 365, 244-260.

Jackson, C. and Spink, A. (2004) User's Manual for the Groundwater Flow Model ZOOMQ3D, IR/04/140, British Geological Survey, Nottingham, UK.

Kelleher, C., T. Wagener, and B. McGlynn (2015), Model-based analysis of the influence of catchment properties on hydrologic partitioning across five mountain headwater subcatchments, Water Resour. Res., 51, 4109-4136.

Kling, H., M. Fuchs, and M. Paulin (2012), Runoff conditions in the upper Danube basin under an ensemble of climate change scenarios. Journal of Hydrology, Volumes 424-425, 6 March 2012, 264-277.

Kollet, S. J., and R. M. Maxwell (2008), Capturing the influence of groundwater dynamics on land surface processes using an integrated, distributed watershed model, Water Resour. Res., 44.

Lehner, B., K. Verdin, and A. Jarvis (2008), New global hydrography derives from spaceborne elevation data, EOS, Transactions, AGU, 89(10), 93-94.

Le Vine, N., A . Butler, N. McIntyre, and C. Jackson (2016), Diagnosing hydrological limitations of a land surface model: application of JULES to a deep-groundwater chalk basin, Hydrol. Earth Syst. Sc., 20, 143-159.

Lee, L. J. E., D. S. L. Lawrence, and M. Price (2006), Analysis of water-level response to rainfall and implications for recharge pathways in the chalk aquifer, SE England, J. Hydrol., 330, 604-620.

Leeper, R., R. Mahmood, and R. I. Quintanar (2011), Influence of karst landscape on planetary boundary layer atmosphere: A Weather Research Forecasting (WRF) model-based investigation, J. Hydrometeorol., 12, 1512-1529.

Ly, S., C. Charles, and A. Degré (2013), Different methods for spatial interpolation of rainfall data for operational hydrology and hydrological modeling at watershed scale. A review, Biotechnol. Agron. Soc. Environ. 17, 392-406.

MacDonald, A. M., L. J. Brewerton, and D. J. Allen (1998), Evidence of rapid groundwater flow and karst type behaviour in the chalk of Southern England, In: Robins, N. S. (ed.) *Groundwater pollution, aquifer recharge and vulnerability*, Geological Society, London, Special publications, 130, 95-106.

Mathias, S. A., A. P. Butler, B. M. Jackson, and H. S. Wheater (2006), Transient simulations of flow and transport in the chalk unsaturated zone, J. Hydrol., 330, 10-28.

Maxwell, R.M. and N.L. Miller (2005), Development of a coupled land surface and groundwater model, J. Hydrometeorol., 6(3), 233-247.

Maxwell, R. M., F. K. Chow, S. J. Kollet (2007), The groundwater-land-surface-atmosphere connection: Soil moisture effects on the atmospheric boundary layer in fully-coupled simulations, Adv. Water Resour., 30, 2447–2466.

Met Office (2006), UK hourly rainfall data, Part of the Met Office Integrated Data Archive System (MIDAS), NCAS British Atmospheric Data Centre, 21 March 2016, http://catalogue.ceda.ac.uk/uuid/bbd6916225e7475514e17fdbf11141c1.

Morton, D., C. Rowland, C. wood, L. Meek, C. Marston, G. Smith, R. Wadsworth, and I. C. Simpson (2011), Final report for LCM2007 – the new UK Land Cover Map (CS technical report no 11/07), Centre for Ecology and Hydrology, UK.

Mu, Q., F. A. Heinsch, M. Zhao, and S. W. Running (2007), Development of a global evapotranspiration algorithm based on MODIS and global meteorology data, Remote Sens. Environ., 111, 519-536.

Price, A., R. A. Downing, and W.M. Edmunds (1993), The chalk as an aquifer. In: Downing, R. A., M. Price, and G. P. Jones *The hydrogeology of the chalk of north-west Europe*. Oxford: Claredon Press. 35-58.

Price, M., R. G. Low, and C. McCann (2000), Mechanisms of water storage and flow in the unsaturated zone of chalk aquifer, J. Hydrol., 54-71.

Rahman, M., M. Sulis, and S. J. Kollet (2014), The concept of dual-boundary forcing in land surface-subsurface interactions of the terrestrial hydrologic and energy cycles, Water Resour. Res., 50, 8531‑8548.

Rahman, M., M. Sulis, and S. J. Kollet (2016), Evaluating the dual-boundary forcing concept in subsurface–land surface interactions of the hydrological cycle, Hydrol. Process.

Hydrol. Earth Syst. Sci. Discuss., doi:10.5194/hess-2016-244, 2016
Manuscript under review for journal Hydrol. Earth Syst. Sci.
Published: 26 May 2016

Rawls, W. J., D. L. Brankensiek, and K. E. Saxton (1982), Estimation of soil water properties, Trans. ASAE, 25(5), 1316–1320.

Robinson, E. L., E. Blyth, D. B. Clark, J. Finch, and A. C. Rudd (2015), Climate hydrology and ecology research support system potential evapotranspiration dataset for Great Britain (1961- 2012) [CHESS-PE], NERC-Environmental Information Data Centre.

Schär C., D. Lüthi, U. Beyerle, and E. Heise (1999), A soil precipitation feedback: A process study with a regional climate model, J. Clim., 12, 722–741.

Schaap, M. G., and F. J. Leij (1998), Database-related accuracy and uncertainty of pedotransfer functions, Soil Sci., 163(10), 765-779.

Sorensen, J. P. R., J. W. Finch, A. M. Ireson, and C. R. Jackson (2014), Comparison of varied complexity models simulating recharge at the field scale, Hydrol. Process., 28, 2091-2102.

Van den Daele, G. F. A., J. A. Barker, L. D. Connell, T. C. Atkinson, W. G. Darling, and J. D. Cooper (2007), J. Hydrol., 342, 157-172.

Van Genuchten, M. Th. (1980), A closed-form equation for predicting the hydraulic conductivity of unsaturated soils, Soil Sci. Soc. Am. J., 44, 892-898.

Walters, D. N., K. D. Williams, I. A. Boutle, A. C. Bushell, J. M. Edwards, P. R. Field, A. P. Lock, C. J. Morcrette, R. A. Stratton, J. M. Wilkinson, M. R. Willett, N. Bellouin, A. Bodas-Salcedo, M. E. Brooks, D. Copsey, P. D. Earnshaw, S. C. Hardiman, C. M. Harris, R. C. Levine, C. MacLachlan, J. C. Manners, G. M. Martin, S. F. Milton, M. D. Palmer, M. J. Roberts, J. M. Rodríguez, W. J. Tennant, and P. L. Vidale (2014), The Met Office unified model global atmosphere 4.0 and JULES global land 4.0 configurations, Geosci. Model Dev., 7, 361-386.

Hydrol. Earth Syst. Sci. Discuss., doi:10.5194/hess-2016-244, 2016
Manuscript under review for journal Hydrol. Earth Syst. Sci.
Published: 26 May 2016

Welliings, S. R., and J. P. Bell (1980), Movement of water and nitrate in the unsaturated zone of upper chalk near Winchester, Hants., England, J. Hydrol, 48, 119-136.

Wetzel P. J., and J.-T. Chang (1987), Concerning the relationship between evapotranspiration and soil moisture. J. Clim. Appl. Meteorol., 26, 18‑27.

Williams, K., and D. Clark (2014), Disaggregation of daily data in JULES (Hadley Centre technical note 96), Hadley Centre, Met Office, UK.

Zehe, E. and G. Blöschl (2004), Predictability of hydrologic response at the plot and catchment scales: Role of initial conditions, Water Resour. Res, 40.

Zehe, E., T. Maurer, J. Ihringer, and E.Plate (2001), Modeling water flow and mass transport in a loess catchment, Phys. Chem. Earth (B), 26, 487-507.

Zehe, E., U. Ehret, T. Blume, A. Kleidon, U. Scherer, and M. Westhoff (2013), A thermodynamic approach to link self-organization, preferential flow and rainfall-runoff behaviour, Hydrol. Earth Syst. Sc., 17, 4297-4322.

Tables

Table 1. Field measurements and remote sensing data.

Data	Spatial scale	Temporal extent	Frequency	Source
Soil moisture	Point[a]	2003-2005	15 day	N. Hewitt (CEH)
Latent heat flux	Global	2006-2011	8 day, 1 month	MODIS
Discharge	Point[b]	2006-2011	1 day	NRFA

[a]Measured at Warren Farm.
[b]Locations are shown in Figure 1a.

Table 2. Hydraulic properties for different soil types (refer to Figure 1c). Saturated hydraulic conductivity (K_s) and porosity data are obtained from *Rawls et al.* [1982]. The Van Genuchten parameters are acquired from *Schaap and Leij* [1998].

Texture	K_s (ms^{-1})	Porosity (-)	α (m^{-1})	n (-)
Loam	3.7×10^{-6}	0.463	3.33	1.56
Silt loam	2.0×10^{-6}	0.50	1.2	1.39
Clay	1.7×10^{-7}	0.475	2.12	1.2

Table 3. Hydraulic properties of chalk.

Properties	Value	Source
K_s (ms^{-1})	1.85×10^{-7}	Price et al., 1993
Porosity (-)	0.40	Price et al., 1993
α (m^{-1})	3.4	Le Vine et al., 2016
n (-)	1.4	Le Vine et al., 2016

Table 4. Comparison between observed and simulated daily average runoff from the two configurations over the Kennet catchment.

Metric	Observed	Simulated (*default*)	Simulated (*macro*)
RR	0.40	0.82	0.38
$\Delta\mu$	-	1.04	-0.07
$\Delta\sigma$	-	2.04	0.56

Hydrol. Earth Syst. Sci. Discuss., doi:10.5194/hess-2016-244, 2016
Manuscript under review for journal Hydrol. Earth Syst. Sci.
Published: 26 May 2016

Hydrology and Earth System Sciences
Open Access
Discussions

Figures

Figure 1. Location (a), vegetation cover (b), and soil texture (c) over the study area. The red line in (a) outlines the Kennet catchment boundary, while the river network is shown in blue. The black triangle in (a) shows the location of the discharge gauging station at the catchment outlet.

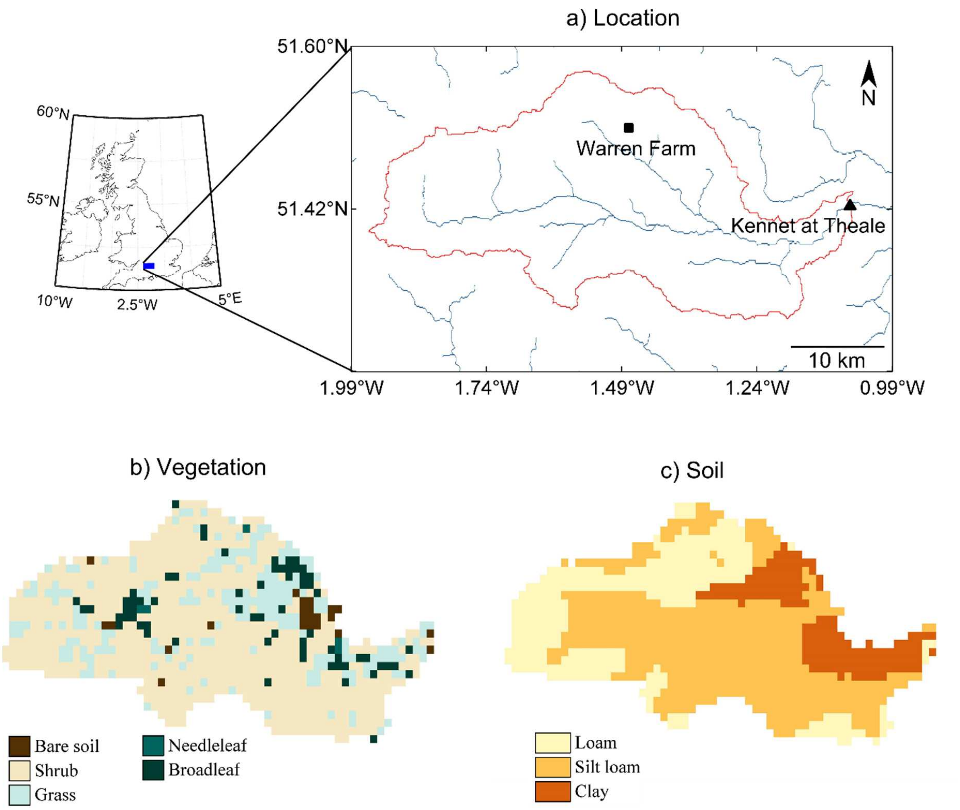

Hydrology and Earth System Sciences
Open Access
Discussions

Figure 2. Example of soil profiles collected at Warren Farm during a field campaign in 2015 (a), and the two model configurations (b).

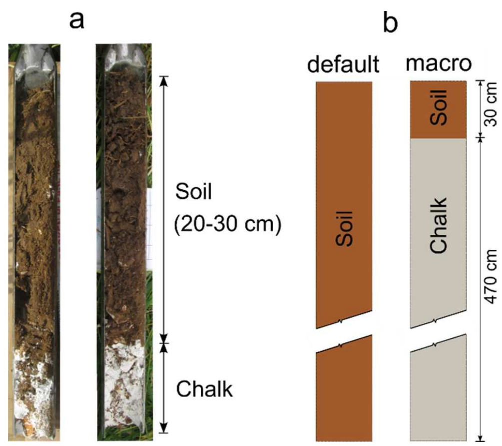

Hydrol. Earth Syst. Sci. Discuss., doi:10.5194/hess-2016-244, 2016
Manuscript under review for journal Hydrol. Earth Syst. Sci.
Published: 26 May 2016

Figure 3. Observed and simulated (*default* configuration) volumetric soil moisture from Warren Farm.

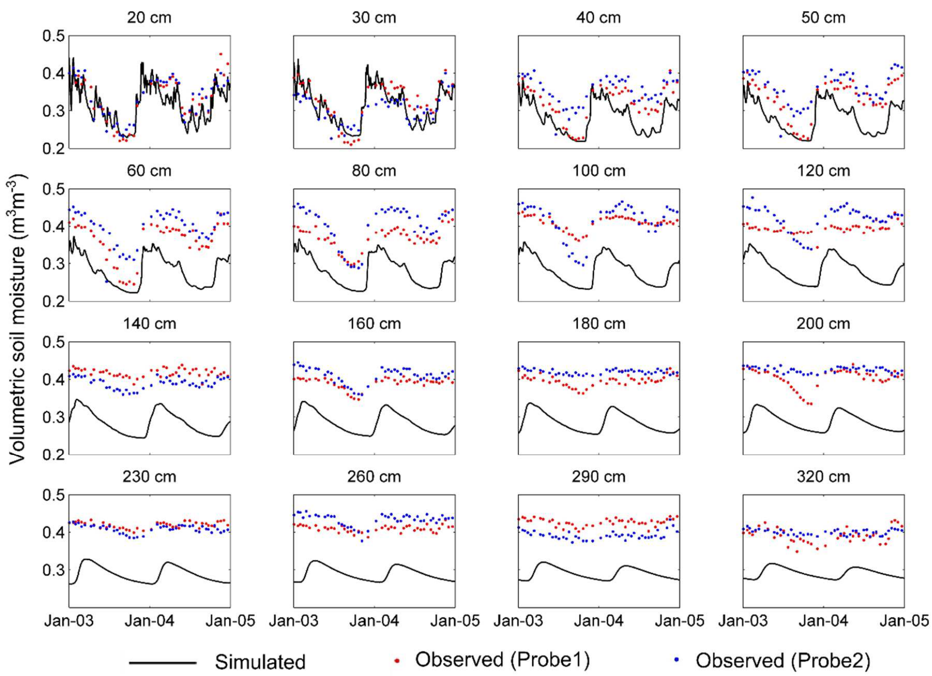

Hydrol. Earth Syst. Sci. Discuss., doi:10.5194/hess-2016-244, 2016
Manuscript under review for journal Hydrol. Earth Syst. Sci.
Published: 26 May 2016

Figure 4. Observed and simulated (*macro* configuration) volumetric soil moisture from Warren Farm.

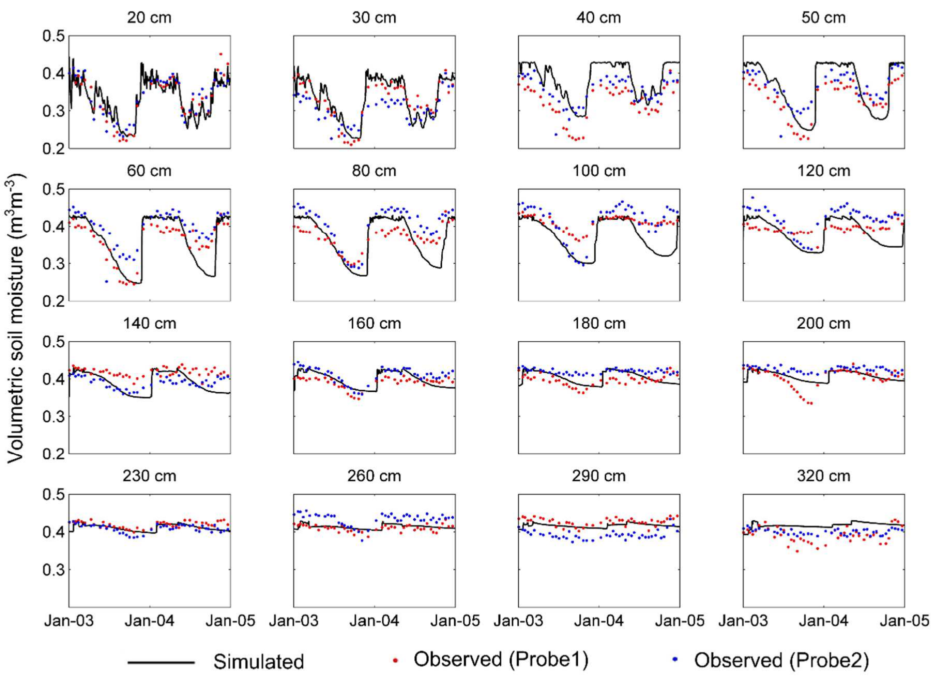

Figure 5. Box plot of relative bias (Δμ) of simulated soil moisture from *default* and *macro* configurations at different depth ranges shown in individual intervals (e.g., 0-30 cm, 30-100 cm, and so on).

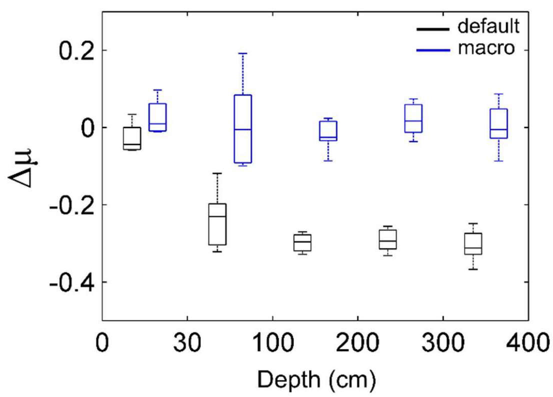

Hydrol. Earth Syst. Sci. Discuss., doi:10.5194/hess-2016-244, 2016
Manuscript under review for journal Hydrol. Earth Syst. Sci.
Published: 26 May 2016

Hydrology and Earth System Sciences
Discussions
Open Access

698 Figure 6. Precipitation (a), daily accumulated downward water flux (w_f, contour lines) plotted
699 over relative saturation (*S*, coloured shading) for *macro* (b), daily accumulated downward
700 water flux plotted over relative saturation for *default* (c), and daily accumulated drainage flux
701 through the bottom boundary simulated by the two model configurations (d) at Warren Farm
702 over the two simulated years (2003-2005).

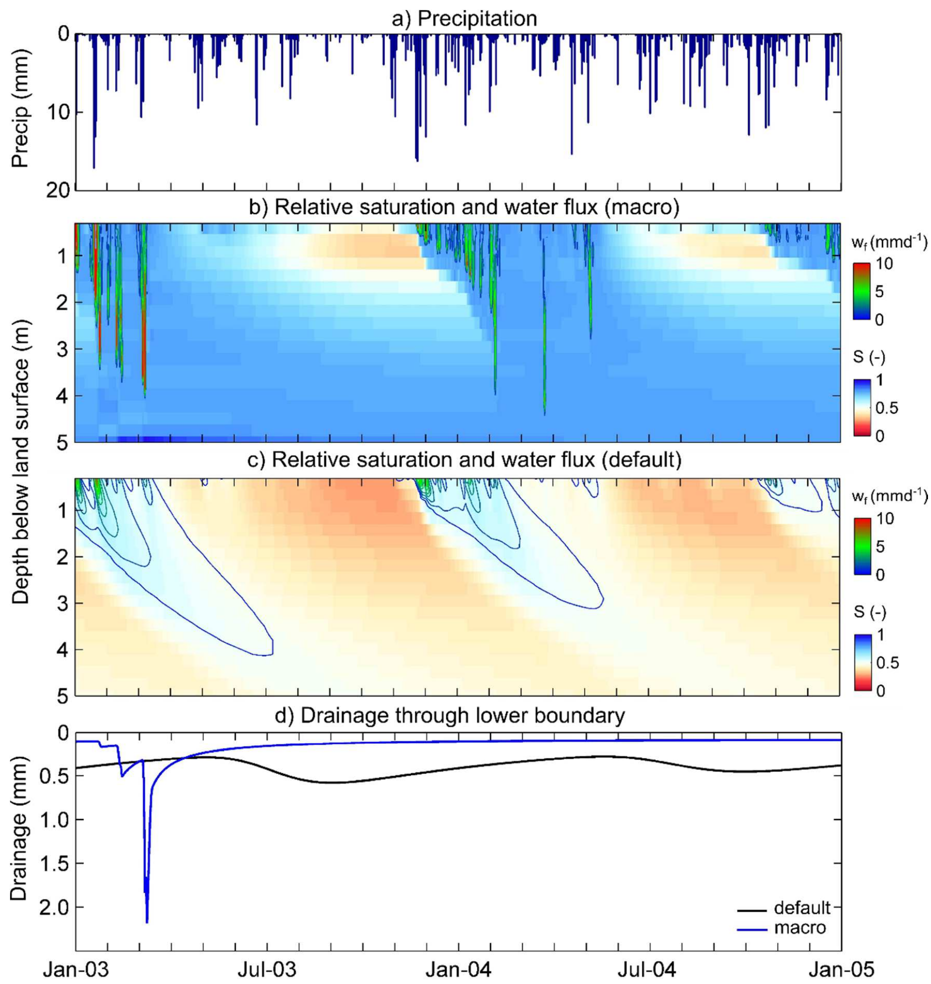

703

704

Hydrol. Earth Syst. Sci. Discuss., doi:10.5194/hess-2016-244, 2016
Manuscript under review for journal Hydrol. Earth Syst. Sci.
Published: 26 May 2016

Figure 7. Differences between daily average latent heat flux time series simulated by *default* and *macro* configurations ($LE_{default}$ and LE_{macro}, respectively) at Warren Farm.

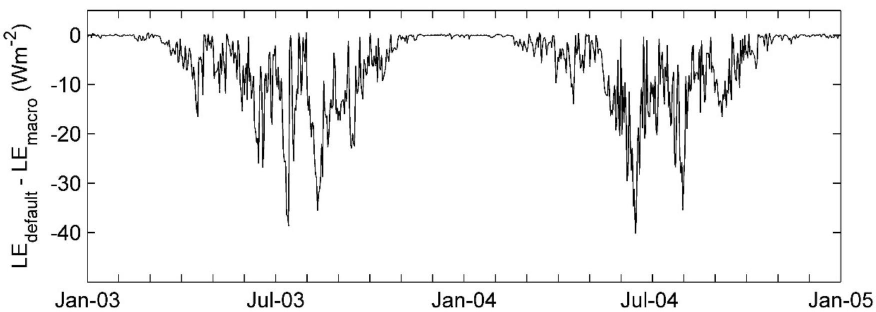

Hydrol. Earth Syst. Sci. Discuss., doi:10.5194/hess-2016-244, 2016
Manuscript under review for journal Hydrol. Earth Syst. Sci.
Published: 26 May 2016

Hydrology and Earth System Sciences
Discussions

Figure 8. Catchment average 8 day composites of MODIS estimated *LE* (LE_{MOD}) against simulated *LE* from *default* and *macro* configurations ($LE_{default}$ and LE_{macro}, respectively) along with the linear models fitted for $LE_{default}$ (black line) and LE_{macro} (blue line). The 1:1 line is shown in red, which represents the perfect fit between LE_{MOD} and simulated *LE*.

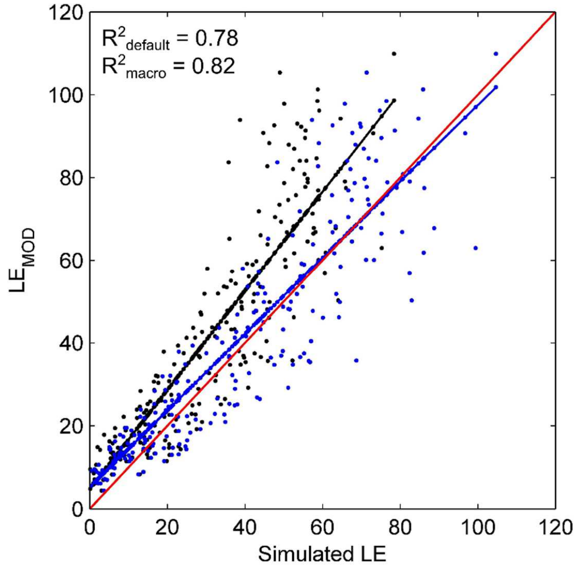

Figure 9. Spatially averaged monthly latent heat flux (*LE*) from MODIS, *default*, and *macro* configurations (a), and average (0-100 cm below land surface) daily relative saturation (*S*) from *default* and *macro* configurations (b) over the Kennet catchment.

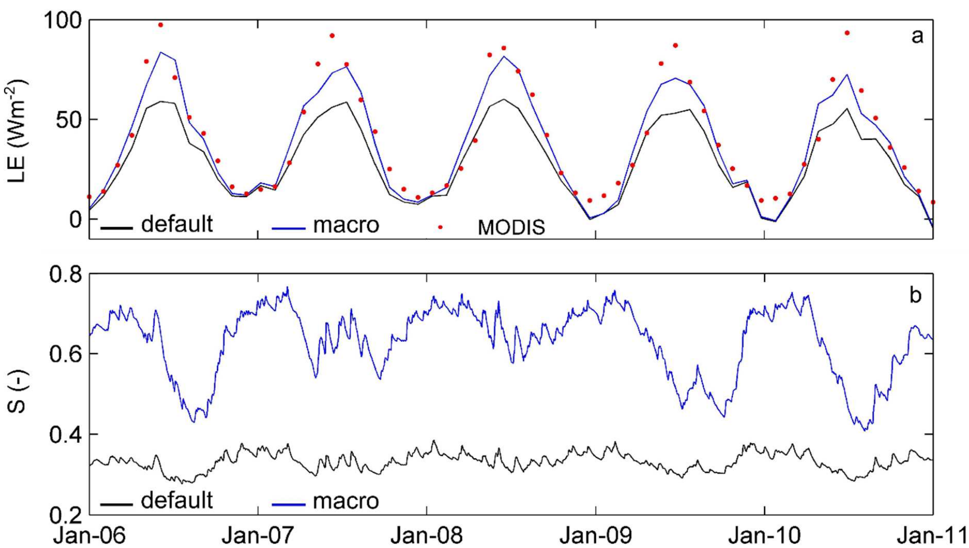

Hydrol. Earth Syst. Sci. Discuss., doi:10.5194/hess-2016-244, 2016
Manuscript under review for journal Hydrol. Earth Syst. Sci.
Published: 26 May 2016

Hydrology and Earth System Sciences
Discussions
Open Access

Supplementary materials

Figure S1. Saturation-pressure head relationship (May 2003 - December 2005) at Warren Farm measured fortnightly at 40 cm below land surface. (Source: Ned Hewett, CEH, personal communication).